

Electronic Supplementary Information

A Li⁺-integrated metallohydrogel based mixed conductive electrochemical semiconductor

Yeeshu Kumar^a and Mrigendra Dubey*^a

^a. *Soft Materials Research Laboratory, Department of Metallurgy Engineering and Materials Science, Indian Institute of Technology Indore, Indore 453552, India.*

Email: mdubey@iiti.ac.in

<u>Table of Contents:</u>	<u>Pages</u>
EXPERIMENTAL SECTION	
Material and physical methods	S2
Rheological Study	S2
EIS Study	S2
Table S1	S3
Synthesis and Characterization	S4
Scheme S1	S5
Supplementary Figures	
Figure S1	S5
Figure S2	S6
Figure S3	S6
Figure S4	S7
Figure S5	S8
Figure S6	S8
Figure S7	S9
Figure S8	S10
Figure S9	S10
Figure S10	S11
Figure S11	S12
Figure S12	S13
Figure S13	S14
Figure S14	S14
Figure S15	S15
Figure S16	S15
Figure S17	S16

EXPERIMENTAL SECTION

Materials and Physical Methods:

Reagents and solvents used in the current research work were procured from Finar Ltd, Ahmedabad, India, S. D. Fine Chem. Ltd, Mumbai, India and used as received without further purification. Methanol was purchased from Advent chembio Pvt. Ltd, Navi Mumbai India. Lithium hydroxide and 5-aminosalicylic acid were procured from Spectrochem Pvt. Ltd., Mumbai (India). Hydrazine hydrate (80%) and $\text{Cd}(\text{CH}_3\text{COO})_2 \cdot 2\text{H}_2\text{O}$ were purchased from Sisco Research Laboratories Pvt. Ltd. Mumbai (India). Terephthalaldehyde was purchased from Sigma-Aldrich.

UV-Vis absorption study was carried on UV2600 Shimadzu spectrophotometer. PerkinElmer's spectrum two spectrometer was used to record FT-IR data. ^1H NMR spectrum was acquired on a AVANCE III 400 and 500 Ascend Bruker BioSpin International AG spectrometer. Electrospray ionization mass (ESI-MS) spectra were recorded on a Waters (Micromass MS Technologies) QToF Premier. FE-SEM images were captured by JOEL-7610 F Plus. Powder XRD data was recorded on Rigaku SmartLab between angle $2\theta = 5\text{--}60^\circ$. TGA experiments were performed using PerkinElmer's STA 8000 simultaneous thermal analyser within the temperature range 30-800 °C and scan rate was kept at 5 °C/min.

FE-SEM sample preparation:

A freshly prepared metallohydrogel (STG) was drop casted on FTO glass substrate and dried at ambient temperature under vacuum for 4 days to obtain dried STG (xerogel). Further, the gold coated STG xerogel sample was mounted to the scanning electron microscope for morphological analysis.

Rheological Study:

Rheological experiments were carried out with the help of a rheometer MCR 102, Anton Paar equipped with stainless steel parallel plates having dimension 20 mm diameter, 1.0 mm gap. Experiments were conducted on freshly prepared gels (2% w/v). Dynamic amplitude sweep experiments were performed to obtain the linear viscoelastic region (LVR) of the metallohydrogel (STG) by determining the storage modulus (G') and the loss modulus (G'') as a function of stress and strain at constant frequency 10 rad/sec, respectively. Dynamic oscillatory frequency sweep was performed at 25 °C (0.1 to 100 rad/sec) at a fixed shear strain of 1%. Time oscillatory strain sweep experiment was conducted at periodic low strain 1% and high strain 100% at constant frequency 10 rad/sec.

Electrochemical impedance spectroscopic (EIS) measurements

Nyquist, Bode impedance plots and Current-voltage characteristic curve

Freshly synthesised metallogel (STG) was casted into a circular shape disc having diameter 1.1 cm and

thickness 0.5 cm. Further, the **STG** disc was sandwiched between two Fluorine-doped Tin Oxide (FTO) electrodes.¹

Nyquist and Bode impedance plots for **STG** were recorded using a CH instruments CHI604E electrochemical workstation within the frequency range 10⁶ Hz to 10⁻² Hz by applying a sinusoidal voltage of 10 mV. The Nyquist plot was fitted with a suitable equivalent electrical circuit model using EIS Analyzer software.^{1,2} The obtained parameters value with error have been listed in table-1.

Table-1: List of obtained parameters values with % error from fitted equivalent circuit model

Parameters	Obtained values from fitted circuit model	% Error
Electronic resistance (R _e)	1.47 x 10 ⁵ Ω	2.97%
Ionic resistance (R _i)	325 Ω	2.45%
CPE ₁	4.94 x 10 ⁻⁹ F.s ⁿ , n = 0.93	4.90%
CPE ₂	2.35 x 10 ⁻⁶ F.s ⁿ , n = 0.85	2.29%

The current voltage characteristics of the **STG** were obtained using a CH instruments CHI604E electrochemical workstation in linear sweep voltammetry mode at a scan rate of 100 mV/sec.^{1,3}

Ionic and electronic conductivity measurements

The ionic and electronic conductivity of **STG** were measured from the conductivity (σ) vs frequency plots (Fig. S11). To obtain σ vs frequency plot the Z' (real component of impedance) vs frequency data were processed by the following equation-

$$\sigma = \frac{1}{R} \cdot \frac{l}{A} \dots \dots \dots (1)$$

Where, R is resistance of the **STG**, l is the distance between two electrodes and A is area of the electrode surface.¹ In σ vs frequency plot, ionic and electronic conductivity of **STG** were measured from high frequency and low frequency plateau, respectively (Fig. S11).^{4,5}

Further, the temperature dependent conductivity experiments were performed in a electrochemical cell and temperature in the cell was controlled by IKA ETS-D5 temperature controller attachment.

Transport number evaluation

The ionic transport number (t_{Li+}) was calculated using the d.c. polarization technique. The electrochemical cell SS| **STG** |SS (SS - stainless steel electrode) was polarized with an applied step potential of 0.75V and resulting current was acquired as a function of time as shown in Fig. S9. The value of t_{Li+} was calculated using the Vincent–Evans equation:

$$t_{Li+} = \frac{I_s(\Delta V - I_0 R_0)}{I_0(\Delta V - I_s R_s)} \dots \dots \dots (2)$$

Where, I₀ and I_s are the initial and steady state current, respectively. R₀ and R_s are the cell resistance before and after polarization experiment obtained with the help of nyquist impedance plot. ΔV represents the applied step potential.⁵

Band gap estimation:

Firstly, diluted metallogel (STG) was dropped onto a precleaned FTO glass substrate. Substrate with diluted STG was placed on the spin coater (Make- Holmarc, Model no-HO-TH-05) and rotated at 1000 rpm for 300 seconds. A STG film was obtained after vacuum drying of the deposited substrate at room temperature for 24 hrs. Further, STG film was subjected to UV-vis spectroscopy to obtain absorption spectrum. To estimate band gap (E_g), we obtained Tauc's plot by processing UV-vis data with following Tauc's equation-

$$(\alpha h\nu)^2 = (h\nu - E_g) \dots \dots \dots (3)$$

Where, α , h , ν and E_g represent, absorption coefficient, Planck's constant, frequency of light and optical band gap, respectively.

Synthesis and characterization:

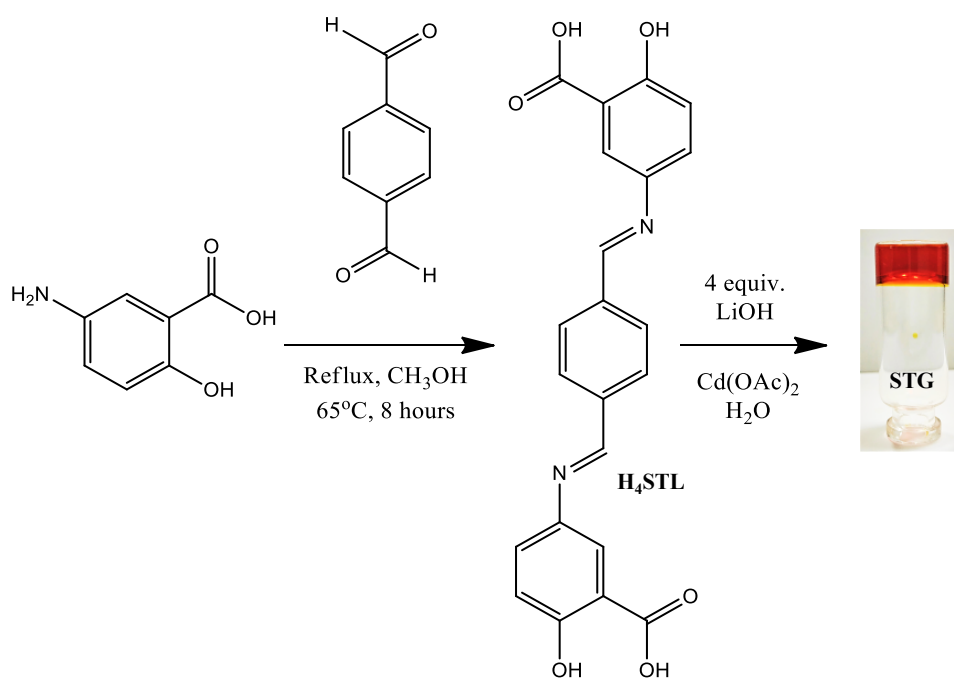
H₄STL gelator molecule

5,5'-((1E,1'E)-(1,4-phenylenebis(methanylylidene))bis(azanylylidene))bis(2-hydroxybenzoic acid)

A methanolic solution of terephthaldehyde (0.5 g, 3.727 mmol) was added dropwise to a solution of 5-aminosalicylic acid (1.141g, 7.454 mmol), and the resulting solution refluxed at 65 °C for 8 hours. The black coloured solid compound was precipitated out from the solution which further subsequently washed with methanol and diethyl ether followed by dried under vacuum. Yield 1.3 g (86%). Anal.calcd.for C₂₂H₁₆N₂O₆: C, 65.34; H, 3.99; N, 6.93; Found: C, 65.15; H; 3.70 N, 6.60. ¹H NMR ((CD₃)₂SO, 500 MHz, δ_H , ppm) 7.04 (d, 2H, Ar-H), 7.61 (d, 2H, Ar-H), 7.78 (d, 2H, Ar-H), 8.06 (s, 4H, Ar-H), 8.78 (s, 2H, -HC=N), 10.09 (s, 2H, -OH), 11.79 (s, 2H, -COOH). ¹³C NMR ((CD₃)₂SO, 400 MHz, δ , ppm) 114.29, 116.31, 117.69, 124.31, 155.07, 172.19, 206.99. ESI-MS *m/z*: [H₄STL.H₂O], 422.17 (*calcd.* 422.17).

Synthesis of metallohydrogel (STG)

H₄STL (20 mg, 0.049 mmol) was suspended in deionised water (0.5 mL) followed by addition of LiOH.H₂O (8.30 mg, 0.197 mmol) and subsequent sonication of the mixture resulted in a dark red coloured solution. A freshly prepared Cd(OAc)₂•2H₂O (13.18 mg, 0.049 mmol) solution in deionised water (0.5 mL) was added to above solution which upon sonication resulted into a red coloured metallohydrogel (STG). The gel formation was primarily confirmed by the inverted vial test method. Anal. calcd. for (C₂₂H₁₂N₂O₆Cd₂Li₂•4H₂O): C, 37.16; H, 2.83; N, 3.94; Found: C, 37.05; H, 2.62; N, 3.80. ESI-MS (diluted gel) *m/z*: [(C₂₂H₁₄N₂O₆Cd•H₂O)+H]⁺, 535.01 (*calcd.* 535.01), [(C₂₂H₁₂N₂O₆Cd₂•H₂O•(LiOH)₂•Na]⁺, 714.91 (*calcd.* 714.91).



Scheme S1: Synthetic route adapted for the synthesis of H₄STL and STG.

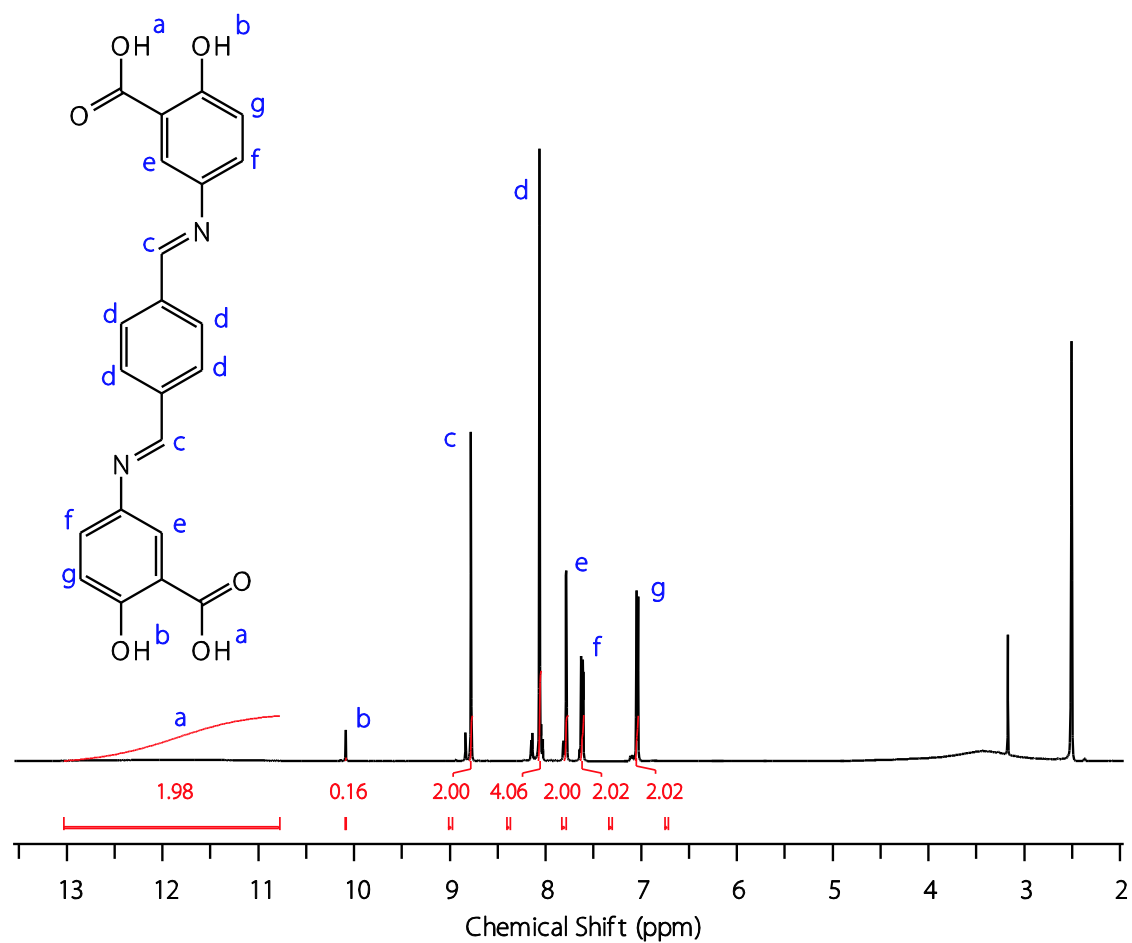


Figure S1. ¹H NMR spectrum of H₄STL (DMSO-d₆, 500 MHz)

Note: Appearance of the additional peaks adjacent to the aldimine and aromatic protons (b to g) suggest the presence of conformers.⁶

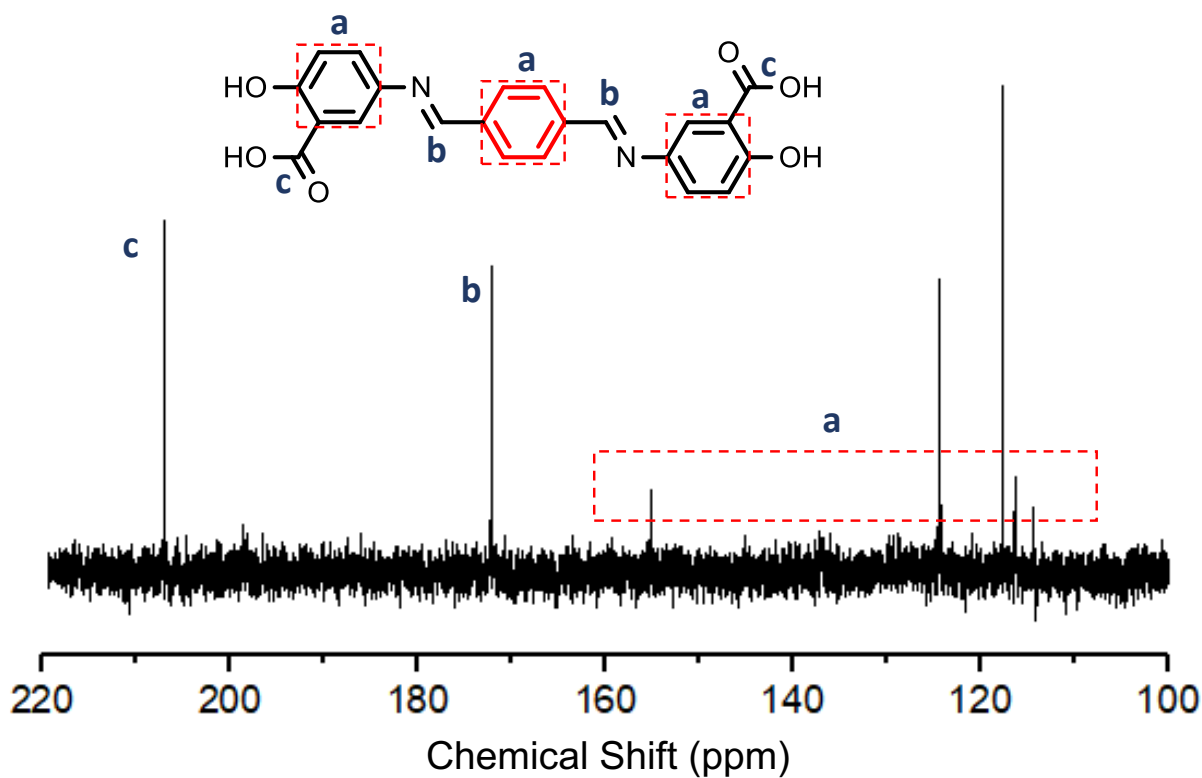


Figure S2. ^{13}C NMR spectrum of H_4STL (DMSO- d_6 , 400 MHz)

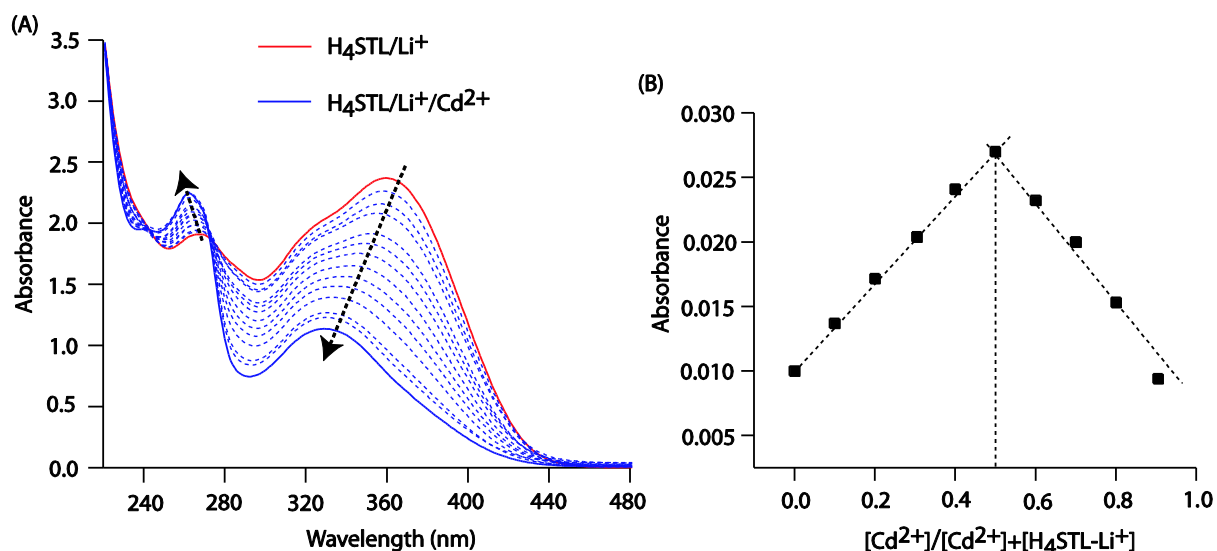


Figure S3. (A) UV-vis titration spectra of H_4STL/Li^+ (1×10^{-4} M, H_2O , red line) vs Cd^{2+} (1×10^{-2} M, H_2O , blue lines) shows isosbestic point at 273 nm which suggests the formation of complex $H_4STL/Li^+/Cd^{2+}$ (B) Job's plot for the 1:1 (Ligand: Metal) complex observed at 460 nm in H_2O .

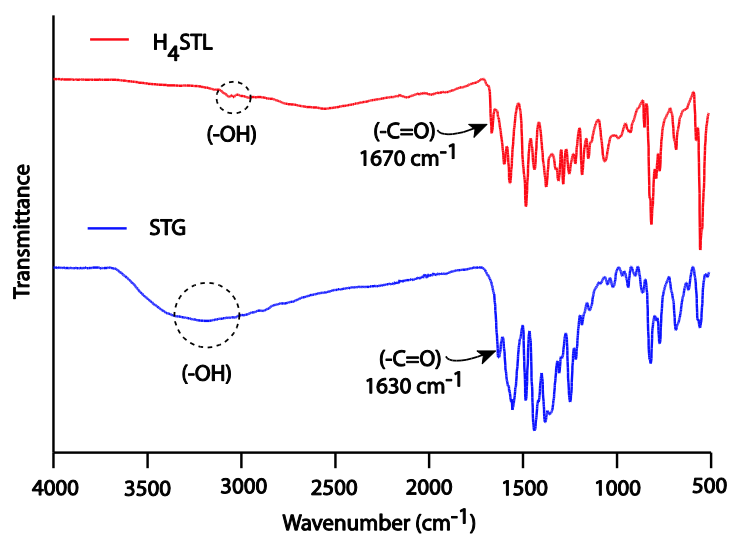


Figure S4. FT-IR spectrum of **H₄STL** gelator (red) shows $\nu(-\text{OH})$ at 3063 cm^{-1} , $\nu(-\text{C}=\text{O})$ at 1670 , 1602 cm^{-1} and $\nu(-\text{C}=\text{N})$ at 1572 cm^{-1} . FT-IR spectrum of **STG** xerogel shows $\nu(-\text{OH})$ at 3233 cm^{-1} , $\nu(-\text{C}=\text{O})$ at 1630 , 1567 cm^{-1} and $\nu(-\text{C}=\text{N})$ at 1557 cm^{-1} .

Note: Broadening of $-\text{OH}$ band in the FT-IR spectrum of **STG** suggests the involvement of H_2O in the coordination complexes, in turn, formation of gel.

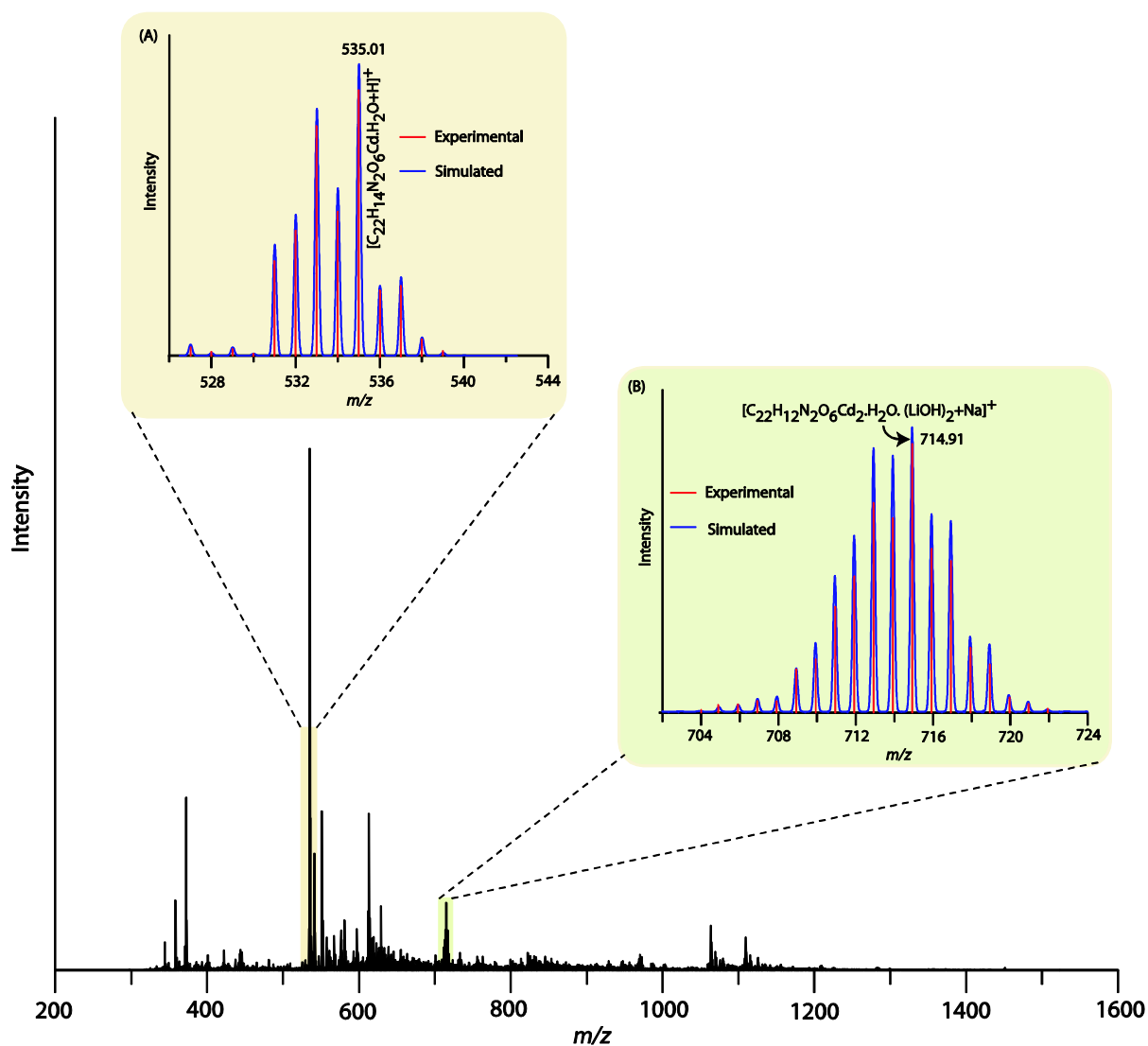


Figure S5. ESI-MS spectra of diluted STG: Isotopic abundance patterns corresponding to the molecular ion species (A) $[C_{22}H_{14}N_2O_6CdH_2O+H]^+$. (B) $[C_{22}H_{12}N_2O_6Cd_2\cdot H_2O\cdot(LiOH)_2+Na]^+$.

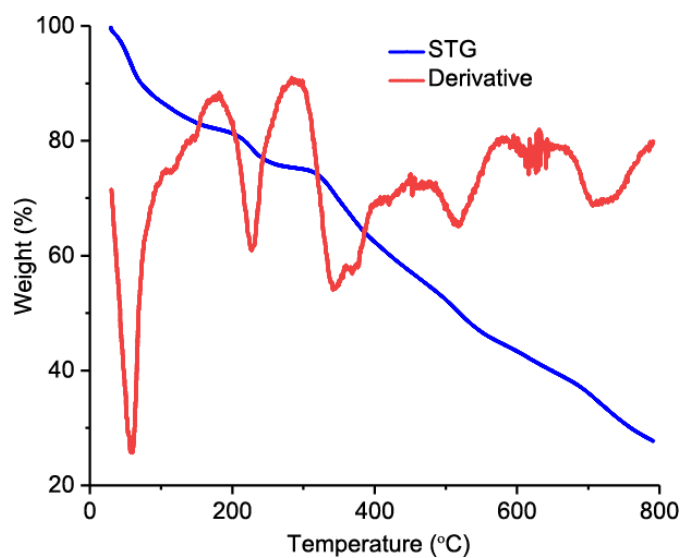


Figure S6. Thermo gravimetric analysis for STG xerogel along with derivative plot.

Note: The weight loss of STG xerogel within the temperature range of 30-300 °C is 25%. The weight loss in this temperature range is due to the removal of free and bound water molecules from the xerogel. Notably, initial weight loss of 13% up to applied temperature 100 °C is accredited to the removal of free water molecules, further weight loss of 12% in the temperature range 100-300 °C is due to removal of bound water molecules thus indicating the coordination of water molecule to the Cd²⁺.¹

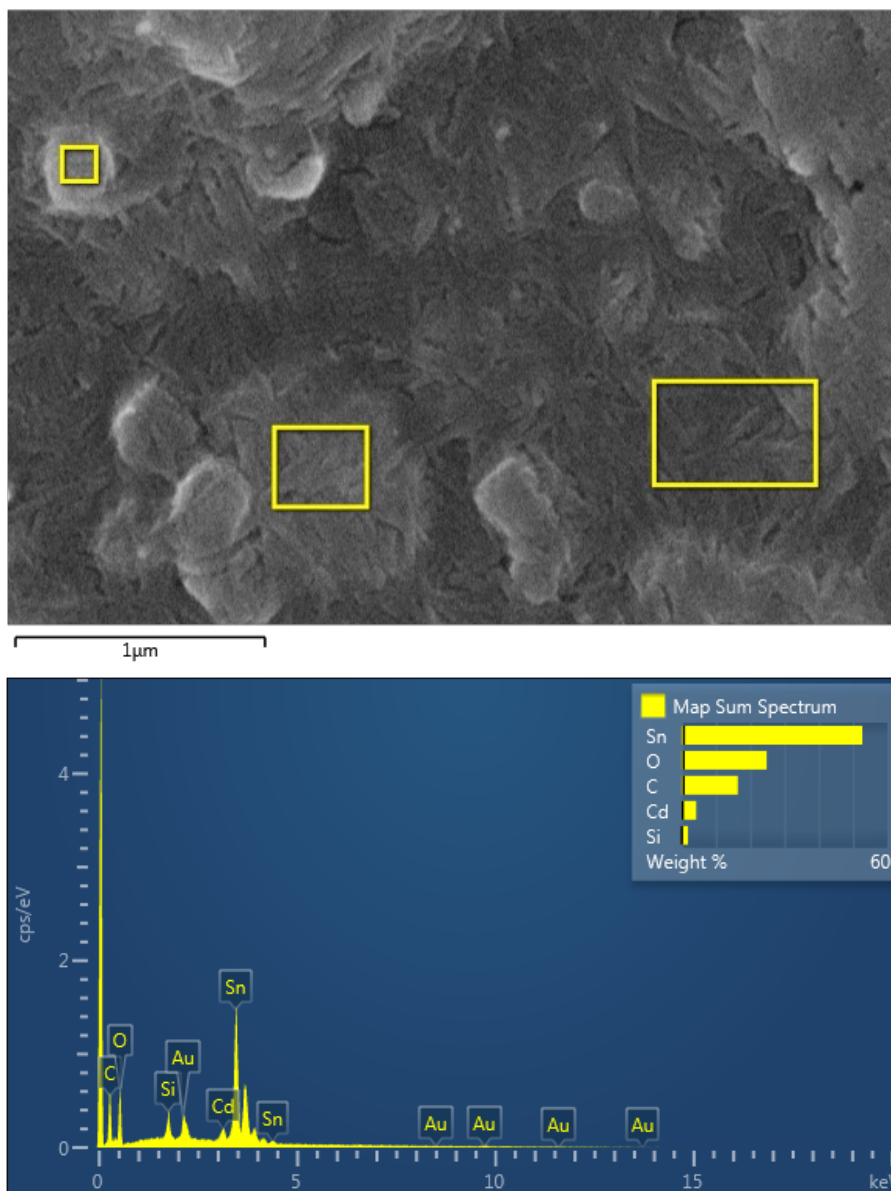


Figure S7. EDS spectrum of STG xerogel showing presence of O, C and Cd elements.

Note: Sn and Si appeared because STG xerogel was deposited on FTO glass, while presence of Au is due to gold coating on the sample.

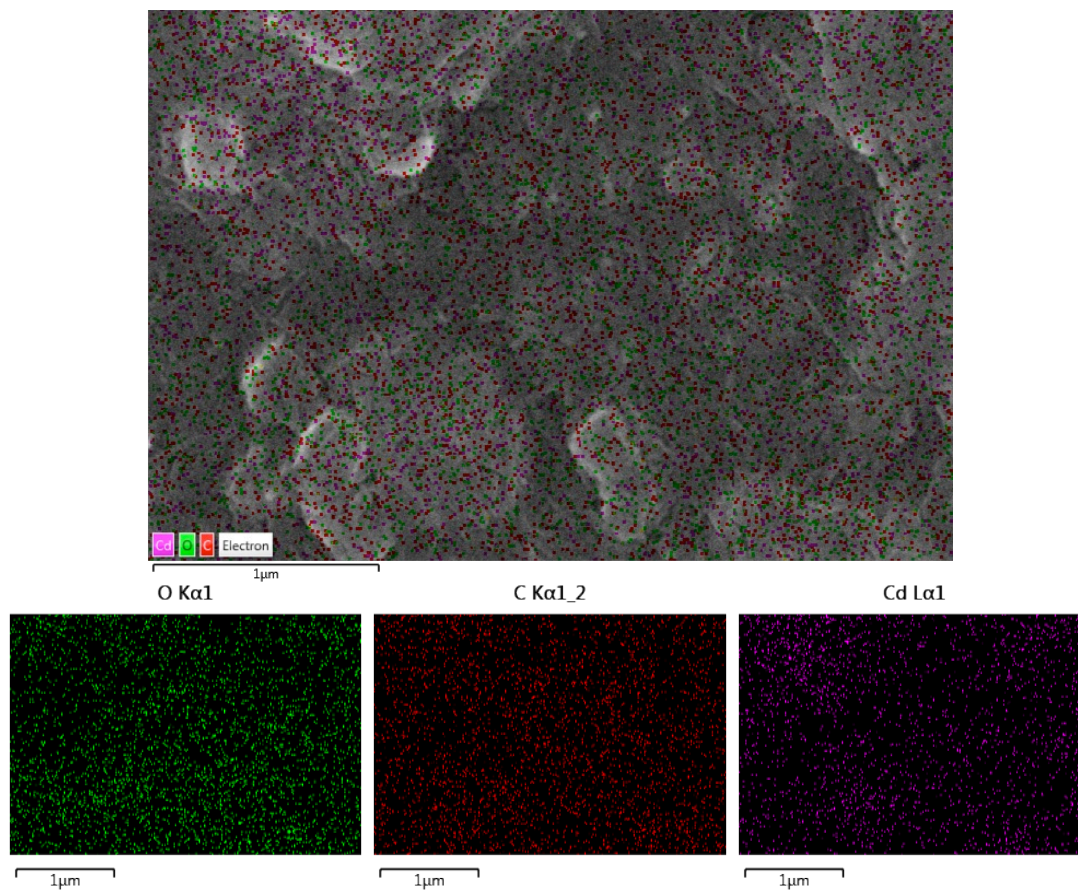


Figure S8. EDS elemental mapping of STG xerogel showing uniform distribution of C, O and Cd elements.

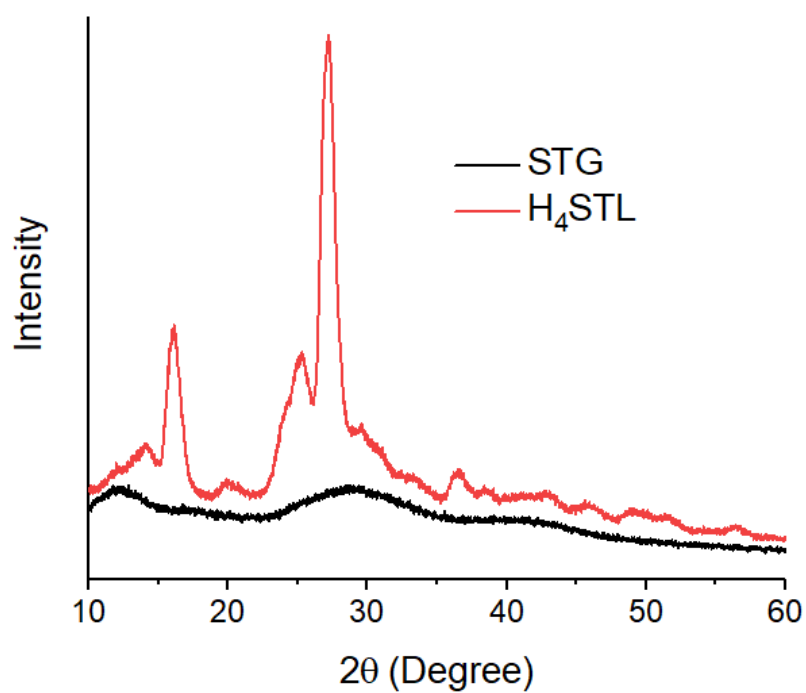


Figure S9. Powder XRD patterns of H₄STL gelator and STG xerogel.

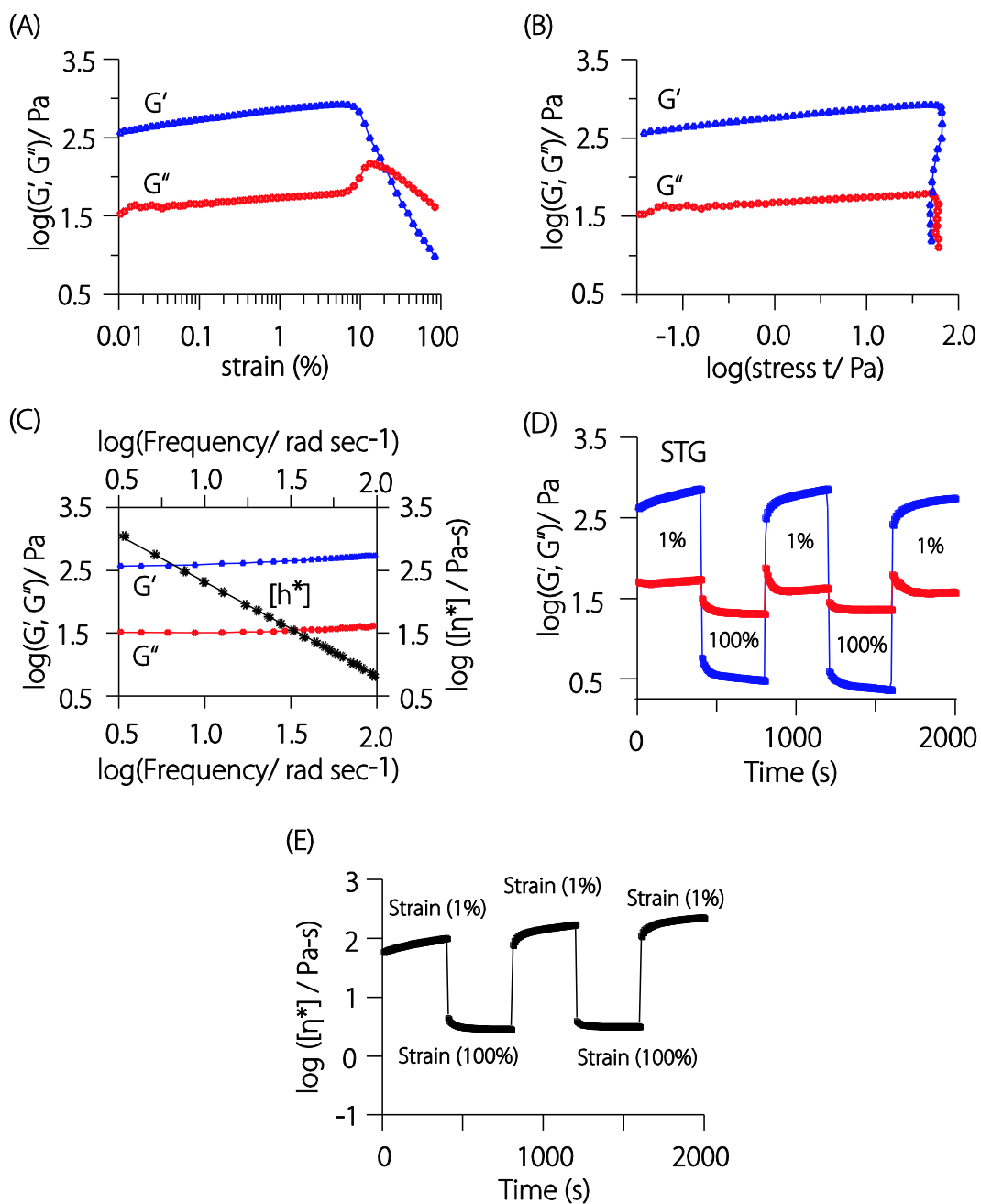


Figure S10. Rheological study over freshly prepared STG metallohydrogel (A) Variation in G' and G'' at a frequency of 10 rad s^{-1} and $25 \text{ }^\circ\text{C}$ under strain sweep, (B) Variation in G' and G'' at a frequency of 10 rad s^{-1} and $25 \text{ }^\circ\text{C}$ under stress sweep, (C) Variation of G'' and G' against oscillatory frequency, (D) logarithmic plots of G' , G'' vs time at periodic strain of 1% and 100%, (E) logarithmic complex viscosity vs time plot at periodic strain of 1% and 100%.

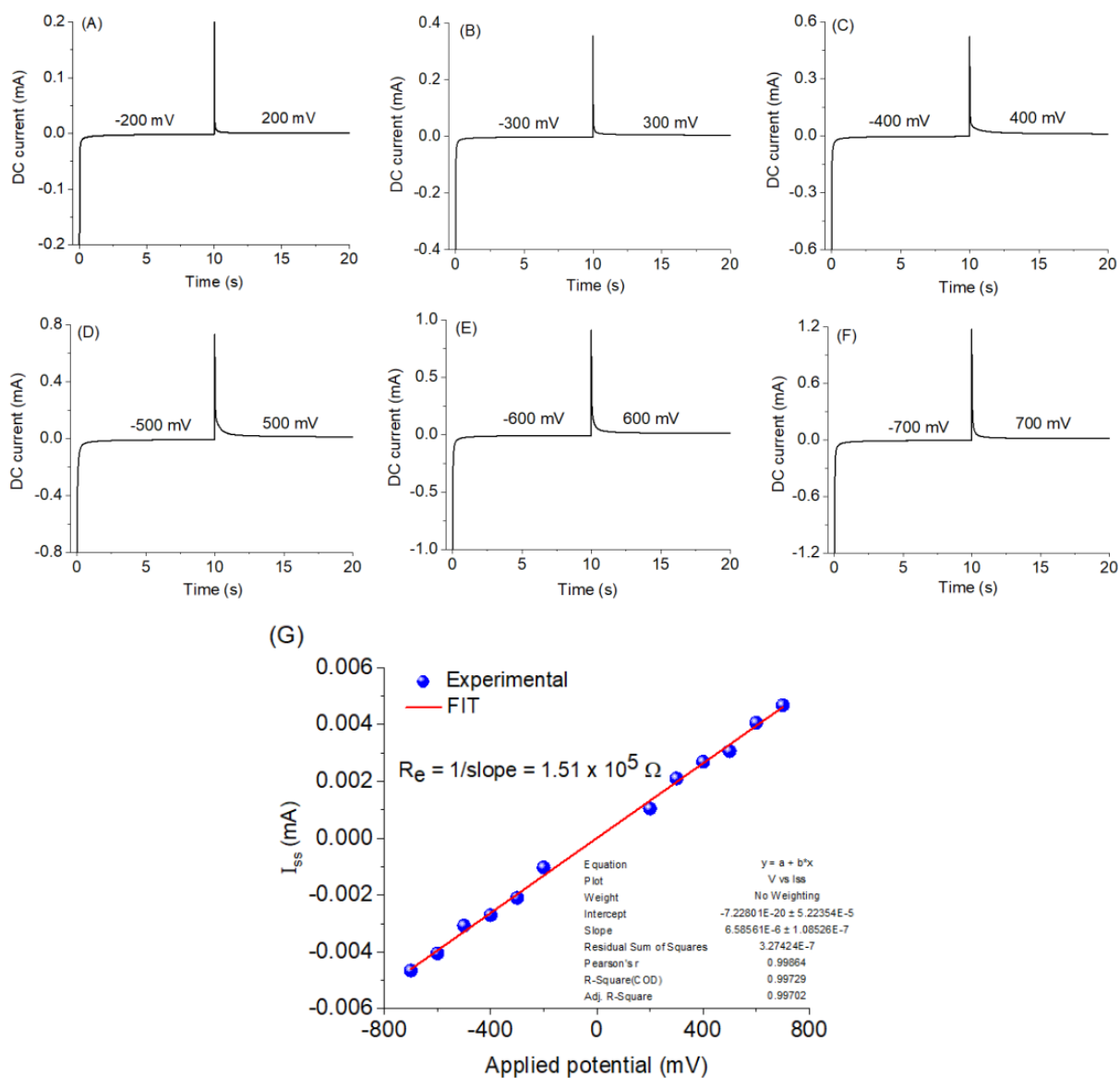


Figure S11. (A-F) DC current vs time curves at different applied DC potentials, (G) Steady state current (I_{ss}) vs applied potential plot, the experimental data follows Ohm's law.

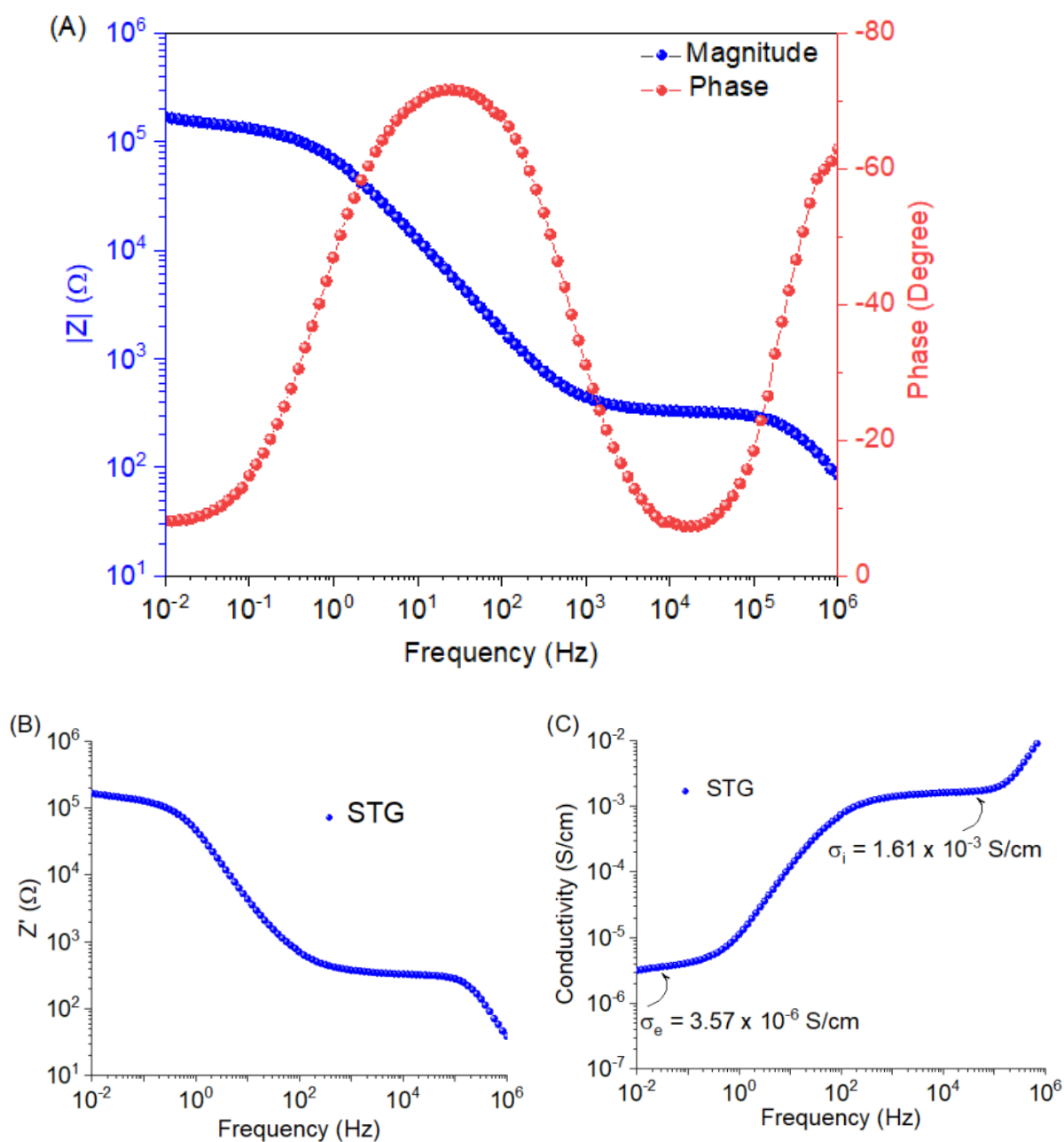


Figure S12. (A) Bode impedance plot for STG, left axis: Bode magnitude plot and right axis: Bode phase plot, (B) Z' vs frequency plot of STG (C) Conductivity vs frequency plot of STG.

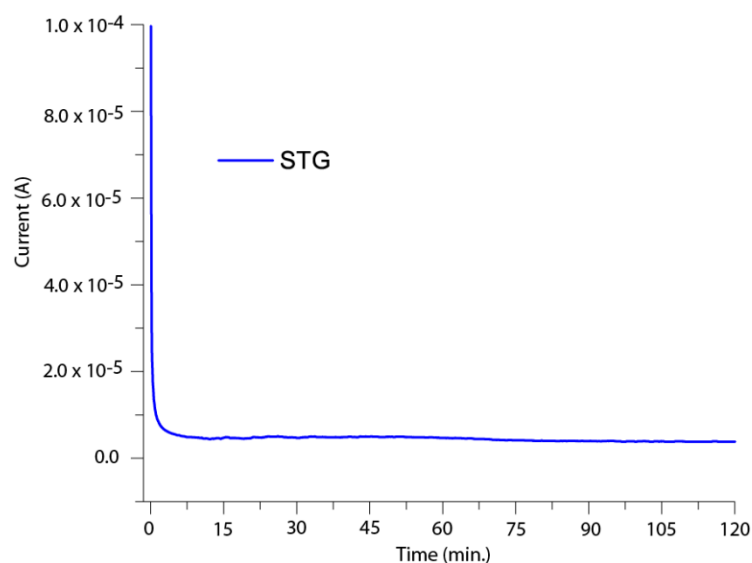


Figure S13. D.C. polarization curve of cell: SS|STG|SS with applied step potential of 0.75 V.

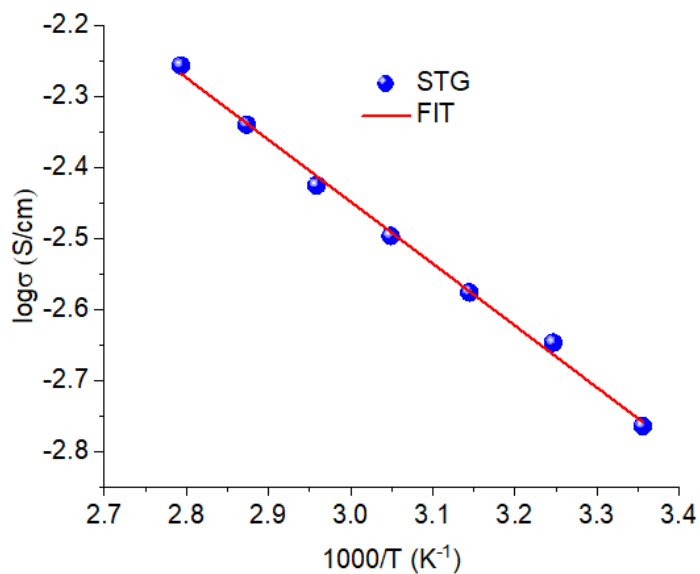


Figure S14. Temperature dependent ionic conductivity plot for STG.

Note- The conductance of the STG was examined by temperature dependent conductivity measurements between the temperature range 298-358 K. The plot of $1000/T$ vs $\log\sigma$ as demonstrated in Fig. S14, the ionic conductivity follows increasing trend with increase in temperature. The enhancement of ionic conductivity is associated with weakening of gel network at higher temperature resulting in the increased mobility of the ionic species within the gel matrix.⁴

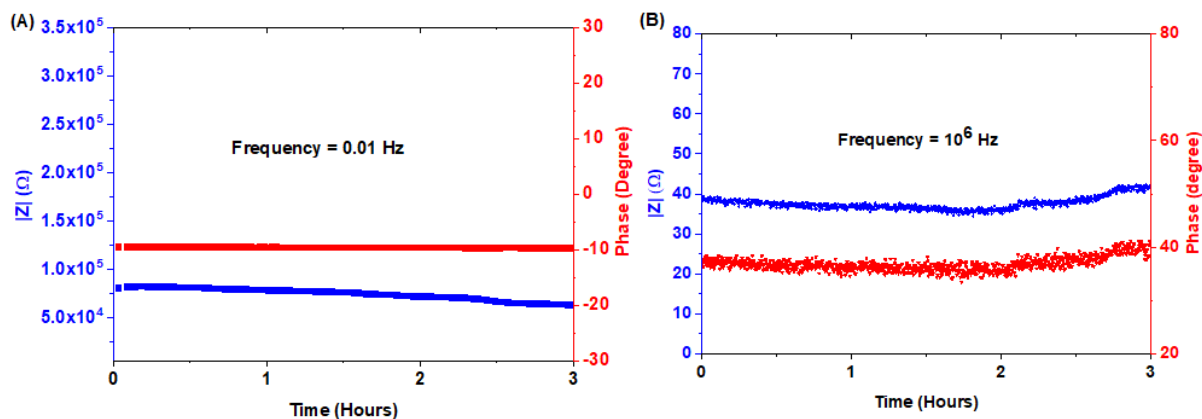


Figure S15. (A) Impedance variation with time at 0.01 Hz and (B) impedance variation with time at 10^6 Hz.

Note- Impedance of STG was monitored for three hours and observed that the impedance showed very slight variation against low and high frequency signal thus revealing electrically stable behaviour of STG.⁵

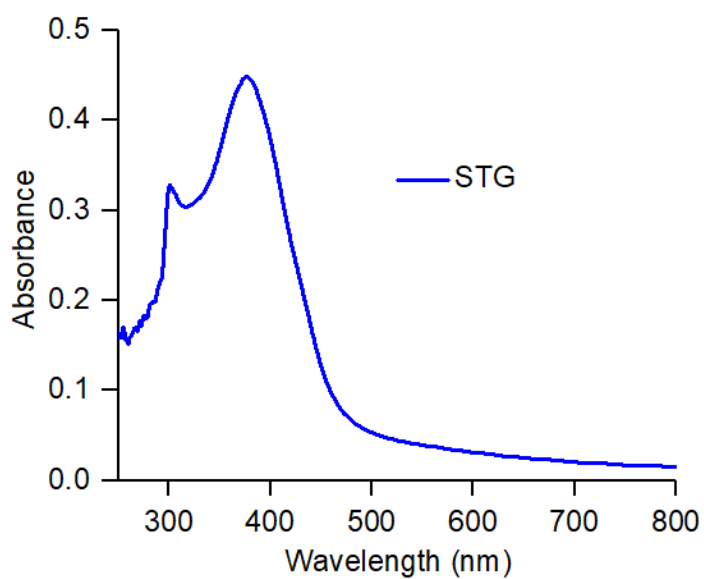


Figure S16. UV-Vis spectrum of STG film deposited on FTO glass.

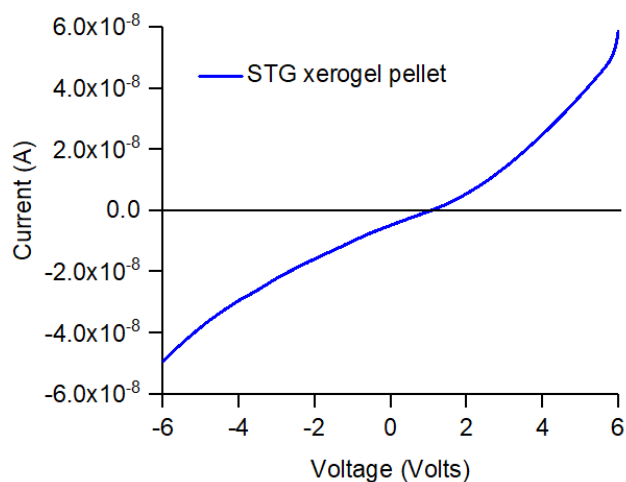


Figure S17. Current-voltage (I-V) characteristic of the STG xerogel pellet.

Note- The STG xerogel provided very small value of current (5.82×10^{-8} A) upon application of 6V bias voltage, which is 5 orders less than the current (1.5×10^{-3} A) obtained for the metallohydrogel.

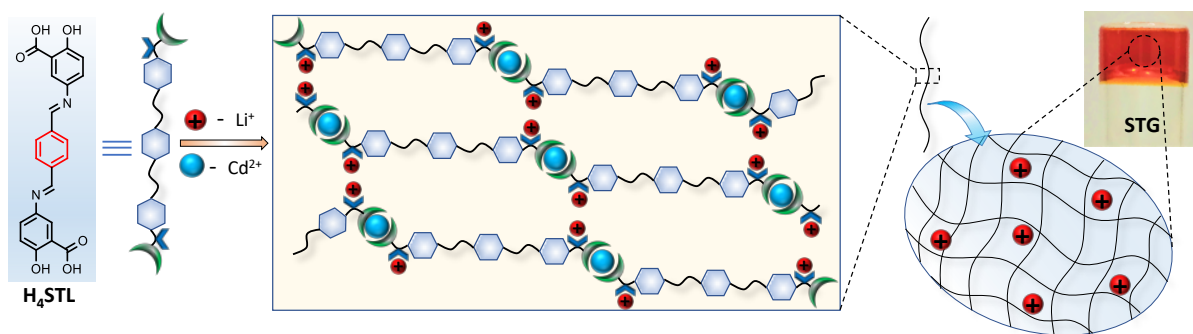


Figure S18. Schematic representation of plausible mechanism for gel formation in STG.

References

1. D. Rawlings et al., *Chem. Mater.*, 2021, **33**(16), 6464.
2. S. N. Patel, A. E. Javier, G. M. Stone, S. A. Mullin and N. P. Balsara, *ACS Nano*, 2012, **6**(2), 1589.
3. K. Nyamayaro, V. Triandafilidi, P. Keyvani, J. Rottler, P. Mehrkhodavandi and S. G. Hatzikiriakos, *Phys. Fluids*, 2021, **33**, 032010.
4. V. K. Pandey, M. K. Dixit, S. Manneville, C. Bucher and M. Dubey, *J. Mater. Chem. A*, 2017, **5**, 6211.
5. Y. Kumar, C. Mahendar, A. Kalam and M. Dubey, *Sustainable Energy Fuels*, 2021, **5**, 1708.
6. M. N. Chaur, D. Collado and J. M. Lehn, *Chem. Eur. J.*, 2011, **17**, 248.